ChemComm

Slow magnetic dynamics in a family of mononuclear lanthanide complexes exhibiting the rare cubic coordination geometry

Journal:	*ChemComm*
Manuscript ID	CC-COM-06-2018-004565.R1
Article Type:	Communication

ChemComm

COMMUNICATION

Slow magnetic dynamics in a family of mononuclear lanthanide complexes exhibiting the rare cubic coordination geometry

Dimitris I. Alexandropoulos,[§] Kelsey A. Schulte,[§] Kuduva R. Vignesh, and Kim R. Dunbar*

Received 00th January 20xx,
Accepted 00th January 20xx

DOI: 10.1039/x0xx00000x

www.rsc.org/

A new family of mononuclear lanthanide complexes, where the eight coordinate lanthanide ions adopt a very rare cubic coordination geometry is reported. The Dy analogue exhibits SMM behavior with a U_{eff} value 95.7 K under a 0.02 T applied *dc* field. Ab initio calculations support the obseved magnetic behavior.

Bistable molecular species that retain their magnetization below a characteristic blocking temperature in the absence of a magnetic field and exhibit magnetic hysteresis loops reminiscent of the diagnostic property of classical magnets are classified as Single Molecule Magnets (SMMs).[1] Slow magnetic relaxation of SMMs originates from an appreciable ground state spin value combined with significant uniaxial magnetic anisotropy (-D_z) which can lead to large energy barriers (U_{eff}) to the reversal of magnetization and high blocking temperatures (T_B).[1b] Experimental detection of the relaxation process is the observation of temperature and frequency dependence of the in-phase (χ′) and the out-of-phase (χ′′) components of the magnetic susceptibility.[1]

Lanthanide complexes have proven to be ideal candidates for SMM behavior due to the fact that most of the rare earth ions, especially Dy^{III} and Tb^{III}, possess remarkably large single-ion anisotropies as compared to other paramagnetic ions of the periodic table.[2] A variety of polynuclear and mononuclear 4*f* metal SMMs have been reported[2] since the first example in 2003[3]. Recently, a highly successful trend in this area of research has been to maximize the axial magnetic anisotropy of individual metal ions by choosing appropriate ligands to affect the strength and the symmetry of the crystal field in low-coordinate systems or highly symmetric coordination environments.[4] The former strategy has produced remarkable results, particularly in the case of the highly sterically congested compound $[(Cp^{ttt})_2Dy][B(C_6F_5)_4]$ (Cp^{ttt}=1,2,4-tri(*tert*-butyl) cyclopentadienide), which exhibits magnetic hysteresis up to 60 K.[5]

Lanthanide ions, however, usually prefer much higher coordination numbers than the aforementioned case, including 8-coordinate species. The most common geometries for 8-coordinate Ln complexes are bicapped trigonal prismatic (C_{2v}), triangular dodecahedral (D_{2d}), and square antiprismatic (D_{4d}) architectures. The latter symmetry is ubiquitous in the field of rare earth SMMs, with an impressive number of bis(phthalocyanine) complexes displaying some of the highest reported energy barriers to date.[3] Although the square antiprismatic geometry is the most prevalent coordination geometry for 4*f* metal ions with eight donor ligands, higher symmetries remain very rare and are largely unexplored vis-à-vis their magnetic properties. In higher symmetries the crystal field parameters responsible for the transverse anisotropy can be minimized thereby improving SMM properties.[2e]

Herein, we report the high-yield syntheses, structures, and magnetic properties of a new family of isostructural mononuclear complexes $[Co^{III}(Tp)_2]_{1.3}[M(NO_3)_2(dbm)_2](NO_3)_{0.3}$ (M = Tb (**1**), Dy (**2**), Er (**3**), and Y (**4**)) with the oxygen donor ligands 1,3-diphenyl-1,3-propanedionate (dbm) and nitrate. The dbm ligand was selected as one of the chelating ligands since β-diketonate complexes have been successfully used in the design of mononuclear Ln SMMs.[6] The diamagnetic $[Co^{III}(Tp)_2]^+$ cation (Tp = tris(pyrazolyl)borate) was generated *in situ* and imposes high crystallographic symmetry and helps to impart greater intermolecular separation between molecules than smaller cations. In these compounds, the eight-coordinate lanthanide ions are in a cubic geometry. These results constitute rare examples in which lanthanide ions exhibit a distorted O_h local symmetry in a LnO_8 coordination environment;[7] the only other related example is $[Dy(ntbi)_2]\cdot 3Cl$ [ntbi = tris(benzimidazol-2-ylmethyl)amine] with a LnN_8 core.[8]

Reactions of $Co(dbm)_2$, $M(NO_3)_3\cdot xH_2O$ (M = Tb^{III}, Dy^{III}, Er^{III}, and Y^{III}), and KTp in a 1 : 1 : 1 molar ratio in MeCN produced pale-yellow/orange crystals of $[Co^{III}(Tp)_2]_{1.3}[M(NO_3)_2(dbm)_2](NO_3)_{0.3}$ (M = Tb (**1**), Dy (**2**), Er (**3**)

‡ *Department of Chemistry, Texas A&M University, College Station, Texas 77842-3012, United States.*
§ D.I.A. and K.A.S. contributed equally to this work
Electronic Supplementary Information (ESI) available: Synthetic, Crystallographic, Computational, and Magnetic details. See DOI: 10.1039/x0xx00000x

and Y (**4**)) (yields >50%) (SI). The chemical and structural identities of the compounds were confirmed by single-crystal X-ray crystallography, elemental analyses (C, H, N), and IR spectral data (SI). The formulae of **1-4** are based on metric parameters, charge-balance considerations, and bond valence sum (BVS) calculations on the Co atom.

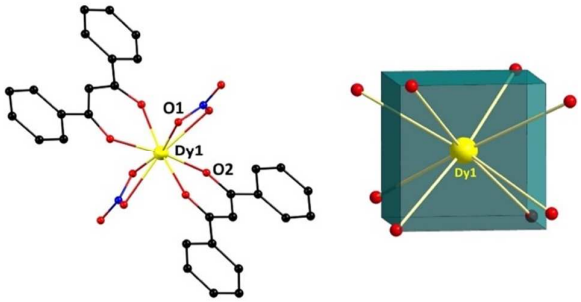

Figure 1. (left) Crystal structure of anion **2** and (right) cubic geometry of Dy1 in the structure of **2**. Points connected by the black lines define the vertices of the ideal polyhedron. H atoms were omitted for the sake of clarity. Color scheme: Dy, yellow; N, blue; O, red; C, black.

In view of the structural similarities of **1**-**4**, only the structure of **2** will be described as a representative example. Complex **2** crystallizes in the cubic space group I23. The asymmetric unit features one quarter of the $[Dy(NO_3)_2(dbm)_2]^-$ anion, with the remainder related through two C_2 axes. There is, also one-third of a $[Co(Tp)_2]^+$ cation, lying on a C_3 axis, and one-third of a disordered nitrate ion in the asymmetric unit. In **2** (Fig. 1) the 8-coordinate Dy^{III} ion is surrounded only by oxygen donor atoms with four coordination sites being occupied by two trans chelating nitrates and the remaining four positions being filled by the O atoms of two chelating dbm ligands. The anion of **2** crystallizes with a $[Co(Tp)_2]^+$ cation (Fig. S2). Charge considerations require a formal Co^{III} description for the cation in **2** which is further supported by the Co-N bond distances (all <1.933(2) Å) which clearly indicate a low-spin Co^{III} ion. The assignment of the Co oxidation state is confirmed by BVS calculations (SI). The crystal packing of **2** (SI) reveals well-isolated $[Dy(NO_3)_2(dbm)_2]^-$ moieties with $[Co(Tp)_2]^+$ cations inserted in between (Fig. S3). The closest intermolecular Dy···Dy contact is 10.453(2) Å.

SHAPE[9] calculations were performed (Table S1) for the Dy1 atom and revealed that it adopts a geometry closest to cubic (CShM: 3.08) (Fig. 1 and Table S2). The two O_4-planes are defined by O1 and O2 atoms with the Dy^{III} ion being centered between the O_4-planes ($d_{Dy\text{-}O4}$ = 1.190(2) Å). The CShM value is large, implying a distorted coordination environment which is further supported by the fact that the Dy-O distances are not equal (2.273(2) Å for Dy-O1 and 2.500(1) Å for Dy-O2) (Fig. 2), indicating deviations from the ideal symmetry.

In order to evaluate the symmetry of the inner coordination sphere around the lanthanide ion in **2**, several key geometrical parameters were evaluated (Fig. 2). Firstly, the angle between the four-fold axis and the Ln-O bond direction (compression angle, θ) that describes the axial distortion of the coordination environment was examined. A value of θ = 54.74° corresponds to an ideal non-distorted cubic environment while smaller or wider angles reflect axial elongation and compression, respectively. [2b, 7b, 10] In **2**, θ was calculated to be 59.59° (average value), revealing axial compression.

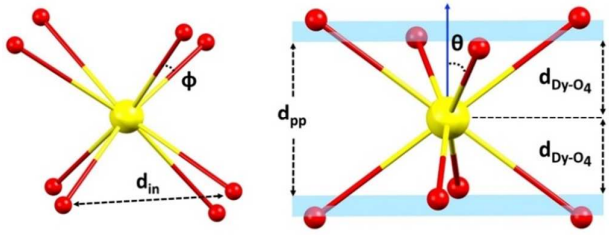

Figure 2. Key geometrical parameters analyzed for the coordination environment of Dy in **2**; see the text for details.

Also, the ratio between the interplanar distance d_{pp} = 2.381(1) Å, between the upper and lower O_4-planes, and the shortest O-O distance in the O_4-plane, d_{in} = 2.905(2) Å, indicates axial compression.[2b, 7b, 10] The d_{in} value is similar to those reported for the axially compressed Ln polyoxometallate complexes LnPOM (2.785-2.964).[7b] Another crucial parameter for the determination of the symmetry of the lanthanide coordination geometry is the skew or twist angle, ϕ, defined as the angle between the diagonals of the two different O_4-planes. A value of ϕ = 0 is expected for an ideal square prismatic or cubic symmetry while a value of ϕ = 45° describes a non-distorted square antiprismatic geometry.[2b, 7b, 10] In **2**, ϕ angle gave an average of 10.22° (calculated as the torsion angle between all different O_4-planes). This value is lower than those reported for the square antiprismatic Ln phthalocyanine $LnPc_2$ (34.4-45)[2b] and Ln polyoxometalate LnPOM (39.1-46.9)[7b] complexes, suggesting that, while the geometry of the Dy ion is very distorted, it is best described as cubic rather than as square antiprismatic (for complexes **1**, **3**, and **4** see Table S3).

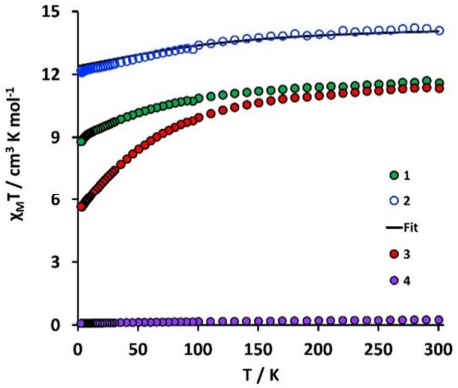

Figure 3. Temperature dependence of $\chi_M T$ for **1**-**4**. Black solid line is the *ab initio* calculated data for **2**.

The static direct current (dc) magnetic properties of **1**-**4** were measured from 2 to 300 K in a 0.1 T applied field (Fig. 3). The data for the diamagnetic complex **4** further support a 3+ oxidation state for the Co ion and confirm that the observed paramagnetic behavior of **1**-**3** arises exclusively from the 4*f* Ln^{III} ions. The experimental $\chi_M T$ values at 300 K for complexes **1**-**3** (11.63 cm^3 K mol^{-1} for **1**, 14.13 cm^3 K mol^{-1} for **2**, and 11.37 cm^3

K mol^{-1} for **3**) are in good agreement with the theoretical values (11.82 cm^3 K mol^{-1} for **1**, 14.17 cm^3 K mol^{-1} for **2**, and 11.48 cm^3 K mol^{-1} for **3**) expected for a single Tb^{III} ($^7F_6$, S = 3, L = 3, g = 3/2) or Dy^{III} ($^6H_{15/2}$, S = 5/2, L = 5, g = 4/3) or Er^{III} ($^4I_{15/2}$, S = 3/2, L = 6, g = 6/5) ion.[11] Complexes **1**-**3** exhibit similar behavior, with χ_MT decreasing slightly from 300 K to reach a value of 10.90 cm^3 K mol^{-1} for **1**, 13.44 cm^3 K mol^{-1} for **2**, and 9.98 cm^3 K mol^{-1} for **3** at 100 K. Below these temperatures, χ_MT decreases more rapidly to a minimum value of 8.84 cm^3 K mol^{-1} for **1**, 12.22 cm^3 K mol^{-1} for **2**, and 5.68 cm^3 K mol^{-1} for **3** at 2.0 K. This steeper decrease observed below 100 K can be mainly attributed to the presence of magnetic anisotropy and/or depopulation of the excited Stark sublevels of the Ln^{III} ions rather than to the presence of intermolecular interactions (average Ln-Ln distance ~10.455(1) Å). This conclusion is further supported by the lack of saturation in the M vs H plots for complexes **1**-**3** (Fig. S4-S6) as well as the fact that the corresponding M vs H/T curves (Fig. S7-S9) are non-superimposed.

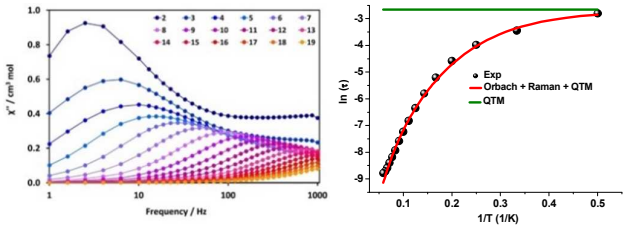

Figure 4. (left) out-of-phase (χ″) component of the magnetic susceptibility vs. frequency, under a 0.02 T applied *dc* field, (right) ln(τ) vs. 1/T plot for complex **2**.

Alternating current (*ac*) magnetic susceptibility measurements were also performed in order to probe the magnetic dynamics of **1**-**3**. Only complex **2** exhibits in-phase (χ′) and out-of-phase (χ″) *ac* susceptibility signals which were frequency and temperature dependent, in the absence of an applied *dc* field (Fig. S14). No peak maxima of the χ″ signals were observed in the frequency range of 1-1000 Hz from 2 to 19 K, indicating significant quantum tunneling of the magnetization (QTM). Such QTM behavior can be suppressed by the application of a small *dc* field. To this end, *ac* susceptibility measurements at various static fields (0 - 0.2T) were performed, and the dc field of 0.02T was chosen as the optimum field at which a well-resolved maximum in χ″ is visible at 10 K (Fig. S11-S12). The presence of peaks that shift to lower frequency as the temperature decreases is indicative of slow magnetic relaxation. At low temperatures, a distinct tail appears at high frequencies, suggesting a second relaxation process. As a result, the experimental data between 2-19 K were fit using a generalized Debye model in CC-fit to extract τ and α parameters with two relaxation processes being considered (Fig. S16). [12] The relaxation times from fitting the main, lower frequency relaxation were plotted as ln(τ) vs. 1/T in Fig. 5. The data in the high-temperature regime, which is dominated by a multi-phonon Orbach process. We were not able to obtain U_{eff} and τ_0 values for the second thermally activated relaxation process since QTM, although reduced to some extent, still dominates the low-temperature regime. To extract an effective energy barrier and to quantify the Raman process, which usually dictates the intermediate regime in the ln(τ) vs. 1/T plot, the data between 2 to 19 K were analyzed by the following equation[13]:

$$\tau^{-1} = \tau_{QTM}^{-1} + CT^n + \tau_0^{-1}\exp\left(-\frac{U_{eff}}{k_BT}\right) \qquad (1)$$

where τ_{QTM}^{-1}, CT^n, and $\tau_0^{-1}\exp(-U_{eff}/k_BT)$ represent QTM, Raman, and Orbach relaxation processes, respectively. A U_{eff}/k_BT of 95.7 K and a pre-exponential factor $\tau_0 = 1.9 \times 10^{-8}$ s were extracted at high-temperatures and the τ_{QTM}^{-1} parameter was obtained as 0.07 s at low-temperatures.[14] Additionally, Eq. 1 gave the following Raman components n = 2.79 and C = 0.98 s^{-1} K$^{-2.79}$.

To further understand the observed magnetic behavior of **2**, CASSCF/RASSI/SINGLE_ANISO *ab initio* calculations were performed, using MOLCAS 8.0 (ESI). These calculations revealed that the ground state Kramers doublet (KD) of the Dy^{III} ion has small transverse components (g_x, g_y), with the g_z value reaching close to the expected value (20) for a pure Ising $|\square_\square = \pm 15/2>$multiplet (Table S5). This indicates a small QTM value for the ground state KD and that magnetic relaxation can occur through higher excited states. The transverse components are enhanced in excited states. Indeed, the second excited KD has larger transverse components, as compared to the first, suggesting that relaxation of magnetization via these KDs is more favorable. This conclusion is in a good agreement with the experimental data where an extremely small dc field is required to attain SMM behavior. The correlation between the *ab initio* computed and the experimental magnetic susceptibility data of **2** (Fig. 3) lends confidence to the extracted parameters.

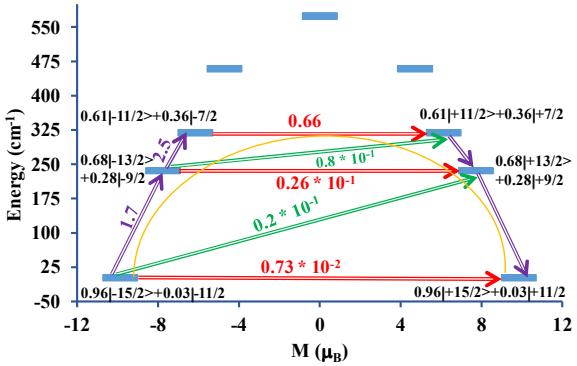

Figure 5. Magnetization blocking barrier for **2**. Thick blue lines indicate Kramers doublets (KDs) as a function of the computed magnetic moment. Green/purple double-dashed arrows show possible pathways through Orbach/Raman relaxations. Double-dashed red arrows represent QTM/TA-QTM between the connecting pairs. The numbers at each arrow are absolute values for the corresponding matrix element of the transition magnetic moment. The yellow curve shows the most feasible magnetic relaxation pathway.

The computed energy barrier was extracted by constructing the magnetic relaxation mechanisms (Fig. 5). In **2**, the ground state axial nature is well reflected in the negligible transversal moment matrix elements relevant to small QTM

process (0.0073 μ_B). This is further supported by the wave function analysis where the ground KD is mostly made up of the $m_J = \pm 15/2 >$ state with small contributions from the $m_J = \pm 13/2 >$ state. Notably, the enhanced transverse first excited KD anisotropy components are supported by considerable transversal moment matrix elements within the first excited state doublets corresponding to the Thermally Assisted-QTM (TA-QTM) process (0.026 μ_B). Additionally, magnetic moment matrix elements related to spin-phonon transitions (direct, Orbach, Raman; green and purple arrows in Fig. 5) between ground and higher excited states (i.e. 1.7/0.02 μ_B) is not sufficient to promote relaxation via the first excited KD. On the other hand, the first excited KD transverse anisotropy is witnessed by enhanced mixed character i.e combination of $m_J = \pm 13/2 >$ and $m_J = \pm 9/2 >$ states. Additionally, the second KD possesses small g_x and g_y components, with a g_z value of approximately 16 indicating presence of strong axial nature even in the first excited energy level. This finding, in conjunction with the small angle between the ground and first excited KDs (0.01°), stimulates relaxation via second excited KDs.[15] The large transverse components ($g_x = 1.89$, $g_y = 2.06$) in the second excited KDs enable fast TA-QTM (0.66 μ_B) between these states. This delineates U_{cal} as 317.6 cm^{-1} (457 K) which is highly overestimated compared to the experimentally determined energy barrier of 95.7 K. This situation is perhaps due to the exclusion of intermolecular and hyperfine interactions in the calculation and the possibility of a non-Orbach relaxation mechanism.[16]

A new family of mononuclear lanthanide complexes in which the metal ions are 8-coordinate, exhibiting a very rare cubic coordination geometry has been isolated but the presence of significant distortions in **1-3**, revealed by the structural analysis, breaks the ideal O_h symmetry of the inner coordination sphere. As a result, slow relaxation of the magnetization at low temperatures was only observed for complex **2** under an applied field of 0.02 T. Fitting of the data, considering all the possible relaxation pathways, gave an energy barrier U_{eff} = 95.7 K with $\tau_0 = 1.9 \times 10^{-8}$ s for the thermal relaxation. *Ab initio* calculations support the SMM behavior of **2**, but overestimate the energy barrier. Work in progress includes substitution of the nitrate ions by other chelating ligands in order to probe how deviations from the cubic symmetry affect the crystal field splitting of the lanthanide ion and the magnetic properties of the compounds.

We gratefully acknowledge the National Science Foundation (CHE-1310574) and Welch Foundation (A-1449) for support. The SQUID magnetometer used was purchased with funds provided by the Texas A&M University Vice President of Research. This research used resources of the Advanced Photon Source, a U.S. Department of Energy (DOE) Office of Science User Facility operated for the DOE Office of Science by Argonne National Laboratory under Contract No. DE-AC02-06CH11357. ChemMatCARS Sector 15 is supported by the National Science Foundation (NSF/CHE-1346572). We are grateful to the HPRC at Texas A&M for the computing resources.

Conflicts of interest

There are no conflicts to declare.

References

1. (a) G. Christou, D. Gatteschi, D. N. Hendrickson and R. Sessoli, *MRS Bulletin*, 2000, **25**, 66-71; (b) R. Bagai and G. Christou, *Chem. Soc. Rev.*, 2009, **38**, 1011-1026.
2. (a) R. Sessoli and A. K. Powell, *Coord. Chem. Rev.*, 2009, **253**, 2328-2341; (b) L. Sorace, C. Benelli and D. Gatteschi, *Chem. Soc. Rev.*, 2011, **40**, 3092-3104; (c) J. D. Rinehart and J. R. Long, *Chem. Sci.*, 2011, **2**, 2078-2085; (d) D. N. Woodruff, R. E. P. Winpenny and R. A. Layfield, *Chem. Rev.*, 2013, **113**, 5110-5148; (e) J.-L. Liu, Y.-C. Chen and M.-L. Tong, *Chem. Soc. Rev.*, 2018, **47**, 2431-2453.
3. (a) N. Ishikawa, M. Sugita, T. Ishikawa, S.-y. Koshihara and Y. Kaizu, *J. Am. Chem. Soc.*, 2003, **125**, 8694-8695; (b) N. Ishikawa, M. Sugita and W. Wernsdorfer, *Angew. Chem. Int. Ed.*, 2005, **44**, 2931-2935; (c) F. Branzoli, P. Carretta, M. Filibian, G. Zoppellaro, M. J. Graf, J. R. Galan-Mascaros, O. Fuhr, S. Brink and M. Ruben, *J. Am. Chem. Soc.*, 2009, **131**, 4387-4396.
4. (a) L. Ungur and L. F. Chibotaru, *Phys. Chem. Chem. Phys.*, 2011, **13**, 20086-20090; (b) N. F. Chilton, D. Collison, E. J. L. McInnes, R. E. P. Winpenny and A. Soncini, *Nature Communications*, 2013, **4**, 2551.
5. (a) F.-S. Guo, B. M. Day, Y.-C. Chen, M.-L. Tong, A. Mansikkamäki and R. A. Layfield, *Angew. Chem. Int. Ed.*, 2017, **56**, 11445-11449; (b) C. A. P. Goodwin, F. Ortu, D. Reta, N. F. Chilton and D. P. Mills, *Nature*, 2017, **548**, 439.
6. (a) S. D. Jiang, B. W. Wang, G. Su, Z. M. Wang and S. Gao, *Angew. Chem. Int. Ed.*, 2010, **49**, 7448-7451; (b) X. L. Li, C. L. Chen, Y. L. Gao, C. M. Liu, X. L. Feng, Y. H. Gui and S. M. Fang, *Chem. Eur. J.*, 2012, **18**, 14632-14637.
7. (a) M. Barsukova, V. Izarova Natalya , N. Biboum Rosa, B. Keita, L. Nadjo, V. Ramachandran, S. Dalal Naresh , S. Antonova Nadya , J. Carbó Jorge , M. Poblet Josep and U. Kortz, *Chem. Eur. J.*, 2010, **16**, 9076-9085; (b) J. J. Baldoví, S. Cardona-Serra, J. M. Clemente-Juan, E. Coronado, A. Gaita-Ariño and A. Palii, *Inorg. Chem.*, 2012, **51**, 12565-12574.
8. S. Goswami, S. Biswas, K. Tomar and S. Konar, *Eur. J. Inorg. Chem.*, 2016, **2016**, 2774-2782.
9. S. Alvarez, P. Alemany, D. Casanova, J. Cirera, M. Llunell and D. Avnir, *Coord. Chem. Rev.*, 2005, **249**, 1693-1708.
10. (a) N. Koike, H. Uekusa, Y. Ohashi, C. Harnoode, F. Kitamura, T. Ohsaka and K. Tokuda, *Inorg. Chem.*, 1996, **35**, 5798-5804; (b) M. A. Sorensen, H. Weihe, M. G. Vinum, J. S. Mortensen, L. H. Doerrer and J. Bendix, *Chem. Sci.*, 2017, **8**, 3566-3575.
11. C. Benelli and D. Gatteschi, *Chem. Rev.*, 2002, **102**, 2369-2388.
12. N. F. Chilton, *CC-fit model*, The Univesity of Manchester.
13. K. R. Meihaus, S. G. Minasian, W. W. Lukens, S. A. Kozimor, D. K. Shuh, T. Tyliszczak and J. R. Long, *J. Am. Chem. Soc.*, 2014, **136**, 6056-6068.
14. A. J. Brown, D. Pinkowicz, M. R. Saber and K. R. Dunbar, *Angew. Chem. Int. Ed.*, 2015, **54**, 5864-5868.
15. T. Pugh, F. Tuna, L. Ungur, D. Collison, E. J. L. McInnes, L. F. Chibotaru and R. A. Layfield, *Nat. Commun.*, 2015, **6**, 7492.
16. K. R. Vignesh, S. K. Langley, K. S. Murray and G. Rajaraman, *Inorg. Chem.*, 2017, **56**, 2518-2532.

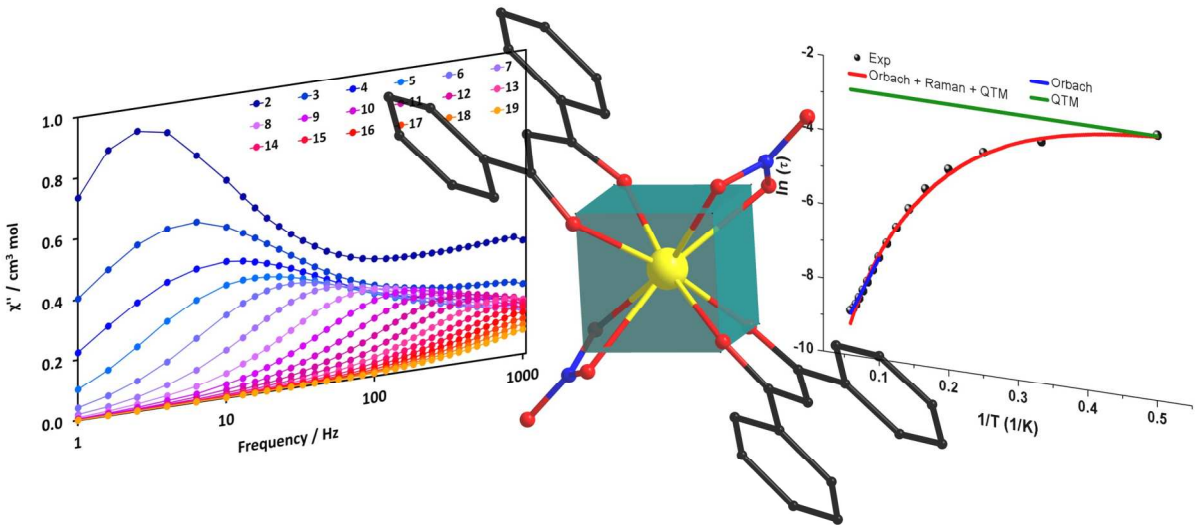

Synthesis, magnetic, and theorecital studies of a new family of mononuclear lanthanide complexes exhibiting the very rare cubic coordination geometry.